Biomatter 2:2, 71–76; April/May/June 2012; © 2012 Landes Bioscience

Synthesis and characterization of biocompatible-nanohydroxyapatite crystals obtained by a modified sol-gel processing

Ignacio A. Figueroa, Omar Novelo-Peralta, Carlos Flores-Morales, Rodrigo González-Tenorio and M. Cristina Piña-Barba*

Instituto de Investigaciones en Materiales; Universidad Nacional Autónoma de México; Circuito Exterior S/N; Ciudad Universitaria; México D.F., México

Keywords: hydroxyapatite, nanocrystals, X-ray diffraction, biomaterials, sol-gel

A modified sol-gel process for synthesizing nanocrystalline hydroxyapatite powders (nHA) for biomedical applications, using tetrahydrated calcium nitrate [$Ca(NO_3)_2{\cdot}4H_2O$] and phosphorous pentoxide [P_2O_5] as precursor, is presented and discussed. The powders were washed and heat-treated at different temperatures and then characterized by X-ray diffraction (XRD), scanning electron microscopy (SEM) and transmission electron microscopy (TEM). The total process time reached with this modified process was less than 16 hours. The results showed that there was an increment in size of the HA nanocrystals (nHA) when treated at different temperatures, ranging from 30 nm for the sample treated at 600°C to 500 nm for the sample heat-treated at 1,200°C.

Introduction

In the past 60 years there have been a number of articles about the importance of hydroxyapatite (HA) as a bone substitute biomaterial. The chemical formula of hydroxyapatite is: $Ca_{10-x}(PO_4)_{6-x}(OH)_{2-x}$; where $1 \geq x \geq 0$; when $x = 0$ is called stoichiometric HA. HA is the main inorganic component of vertebrate bones and the main factor of the hardness and strength of bones and teeth. It forms the enamel of each tooth, which is the hardest material known in animals due to the arrangement of HA crystals in the teeth.[1-7] This material has been reported in many different ways, i.e., as solid, crystalline or amorphous powder and coating. In the last years, its application has been focused as HA nanocrystals (nHA) for bone implants, as composite polymeric biocompatible fibers, as a coating on titanium prosthesis,[8,9] as well as in the drug delivery field.[10-17] When the HA is implanted, the processes of resorption, osteoconduction and bioactivity may occur, which make it very valuable for medical purposes. Due to these properties, it is also used as a bone substitute in cavity filling, coating of metal implants and reinforcement in composite materials.[8]

HA is synthetically obtained in the laboratory by several methods, such as hydrothermal process, precipitation and sol-gel, among others, and depending on the applications, some characteristics such as bioactivity, crystal size and composition can be determined by controlling the main variables from the beginning the process,[16] i.e., reagents, temperature, reaction time, pressure and experimental process.

The most common method to obtain HA is the precipitation method,[18-20] since large amounts of material could be collected; it is inexpensive and easily reproducible. On the other hand, sol-gel processing offers the potential to reliably produce ceramic films and bulk forms through the careful control of the initial suspension "structure" and its evolution during fabrication.[1,21-23] This approach involves five basic steps: (1) powder synthesis, (2) suspension preparation, (3) consolidation into the desired component shape, (4) removal of the solvent phase and (5) densification to produce the final microstructure required for optimal performance. The objective of this work is to produce, through a modified sol-gel approach, nHA for medical applications. It is also worth mentioning that this research is also looking into reducing the synthesis time and the possibility of controlling the final crystal size.

Results

When adding P_2O_5 to ethanol a clear solution was obtained. During this process, a white gas—like fog—on top of the liquid was observed, followed by an increment in temperature; this means that an exothermic reaction has occurred. When adding $Ca(NO_3)_2$-$4H_2O$ to ethanol a clear solution was also obtained. In the final solution, a slow formation of white filaments was observed. After one hour of agitation, the mixture had a white, homogeneous and opaque appearance with much higher apparent viscosity than the initial mixture.

When the mixture was dried, the material obtained looked very similar to white foam, with homogeneous porosity, as shown in **Figure 1**. The color of the heat-treated crystalline samples varied as the temperature increased, it changed from gray to bluish white. All samples resulted with a fine grain texture very similar to the texture of talc; the total process time was 16 h.

*Correspondence to: M. Cristina Piña-Barba; Email: mcpb@unam.mx
Submitted: 10/31/11; Revised: 04/11/12; Accepted: 04/13/12
http://dx.doi.org/10.4161/biom.20379

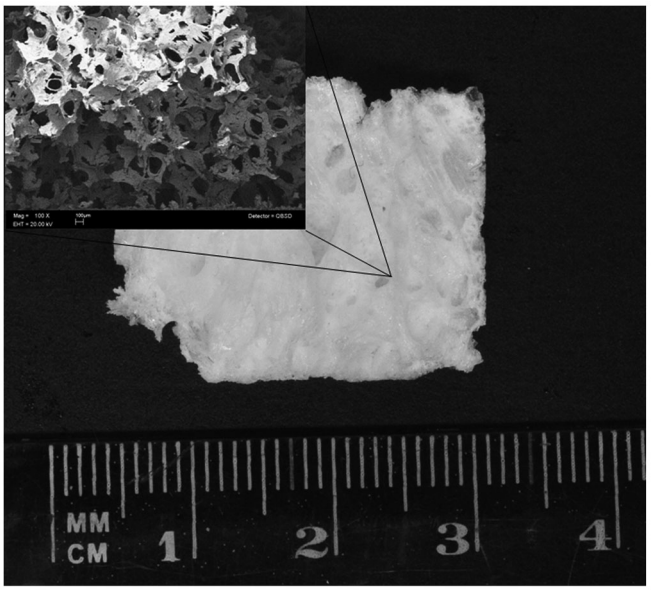

Figure 1. HA open-celled foam obtained after the drying process.

Figure 2 shows the XRD traces for the sample shown in **Figure 1**. The XRD patterns of the heat-treated samples at 600°, 900° and 1,200°C are shown in **Figure 3**. These XRD patterns revealed the formation of the crystalline phase corresponding to HA, which is the main component. Besides, there was evidence of the presence of a small trace of calcium phosphate, which is generally known as Whitlockite.

Figures 4, 5 and 6 show the bright field TEM images of the heat-treated samples and their corresponding electron diffraction patterns, respectively. The electron diffraction patterns correspond to the XRD observed nHA phase. These figures clearly show the increment in size of the nHA when treated at different temperatures. After heating at 600°C, the average size particles range from 30 to 50 nm, showing a regular shape and no porosity (**Fig. 4**). When the heating temperature rose up to 900°C (**Fig. 5**), the size of the particles increase up to 150 nm. Finally, at the highest heat treatment temperature at which this material was treated, 1,200°C, the final particle size was 500 nm, as shown in **Figure 6**.

During determination of surface area, the adsorption isotherm of nitrogen was also obtained for hydroxyapatite. **Figure 7** shows the isotherm adsorption of the nHA sample heat-treated at 600°C. The surface area of nHA samples heat-treated at 600°C, 900°C and 1,200°C was 7.0 ± 0.7, 6.4 ± 0.5 and 2.3 ± 0.2 $m^2 g^{-1}$, respectively.

Discussion

It is believed that the process of nucleation and initial growth of colloidal nanocrystals strongly depends on the rise of the concentration of the ions in the solution; consequently, the kinetics of nucleation of the spherical colloidal particles is controlled by the evaporation of the solvent used in the experiment (ethanol). Therefore, as the solvent is evaporated, the concentration of ions increases, producing the nucleation. The nucleation period is limited to a short period of time, and the growth (agglomeration of nanoparticles) is also induced, initially, by the evaporation of the ethanol. It is worth mentioning that the size of these

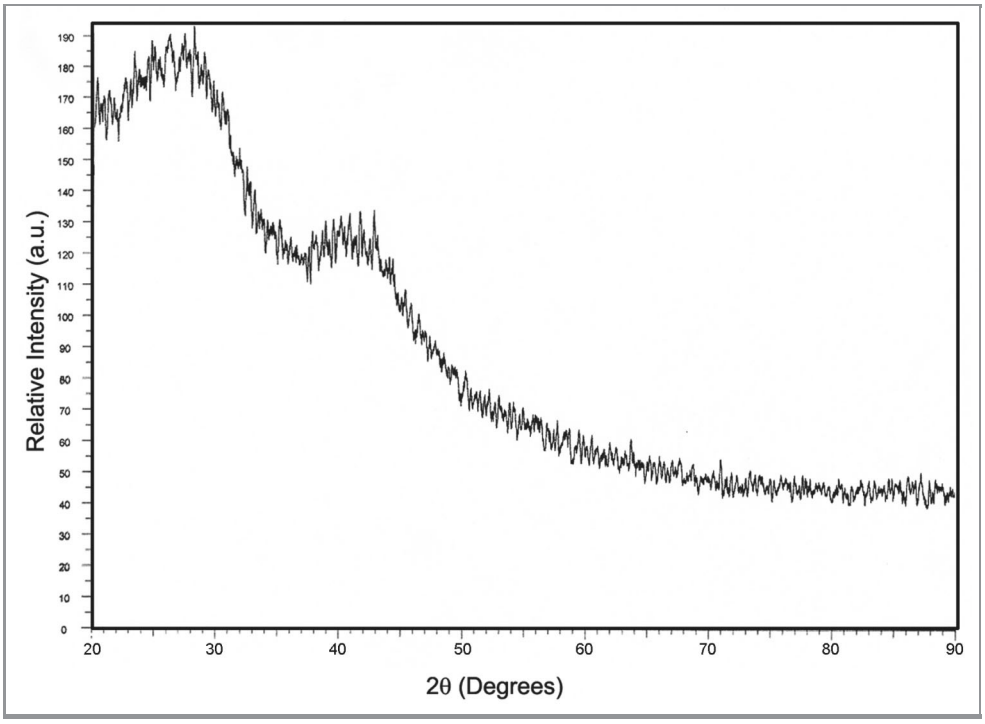

Figure 2. XRD pattern for the HA open-celled foam obtained after the drying process.

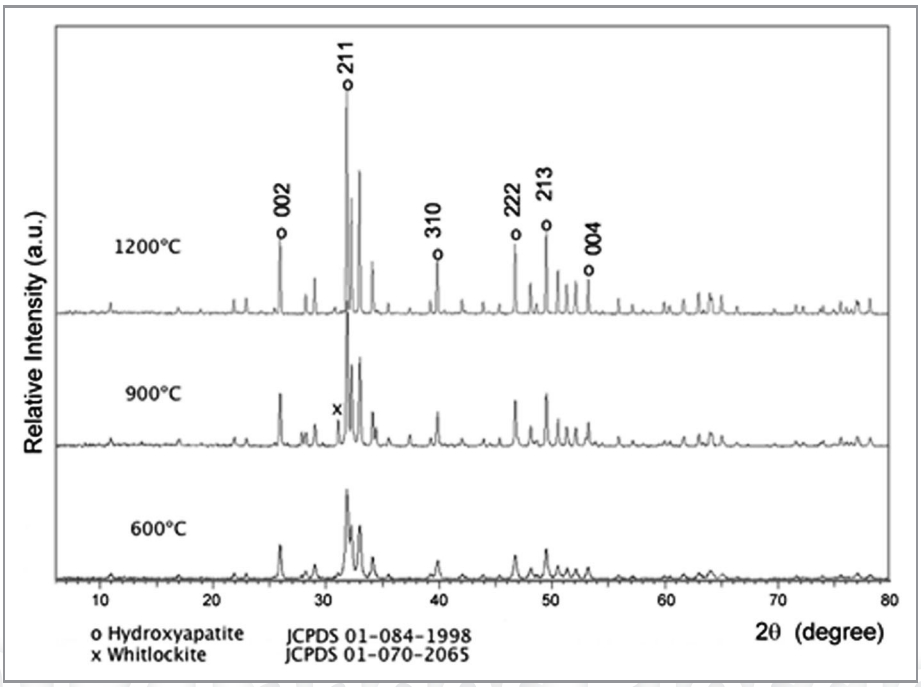

Figure 3. XRD pattern for the HA heat-treated at different temperatures.

agglomerates or nanoparticles is too small to be detected by XRD, producing an amorphous-like pattern, as shown in **Figure 2**. With the heat treatments, the energy barrier required for the formation of new surface area was overcome and the growth of the nanoparticles formed during the synthesis was observed. The heat treatment process provides energy to the system, promoting the rearrangement of the crystals formed in a configuration of lower energy, helping the growth of the crystals.

From XRD patterns, it can be observed that as the heat treatment temperature increases, the diffraction peaks become

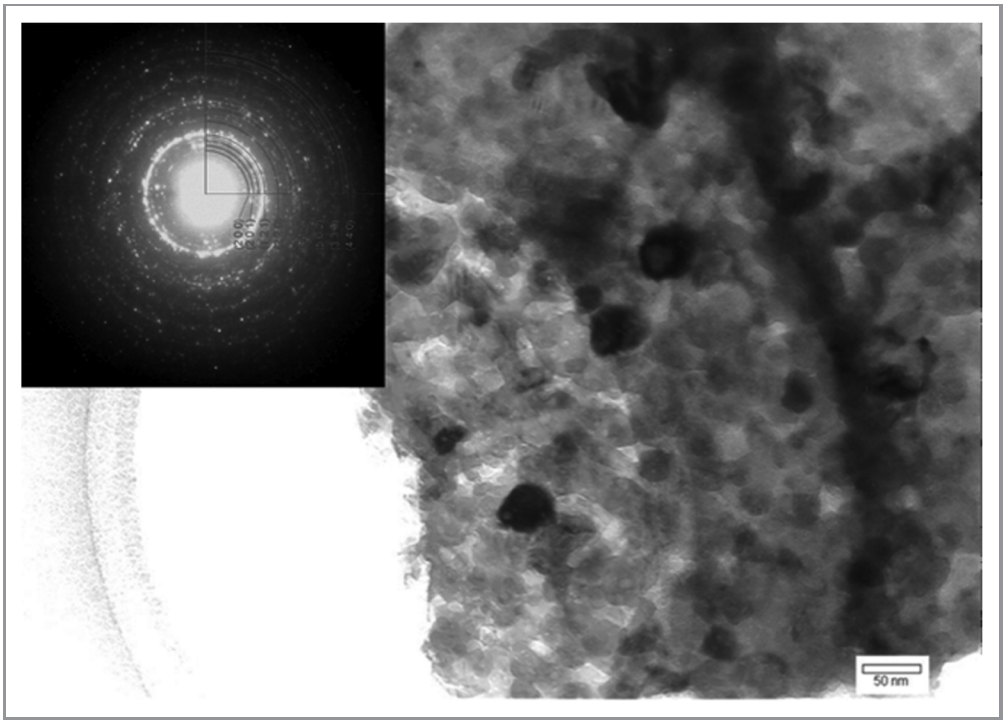

Figure 4. TEM bright field image and electron diffraction for the HA heat-treated at 600°C.

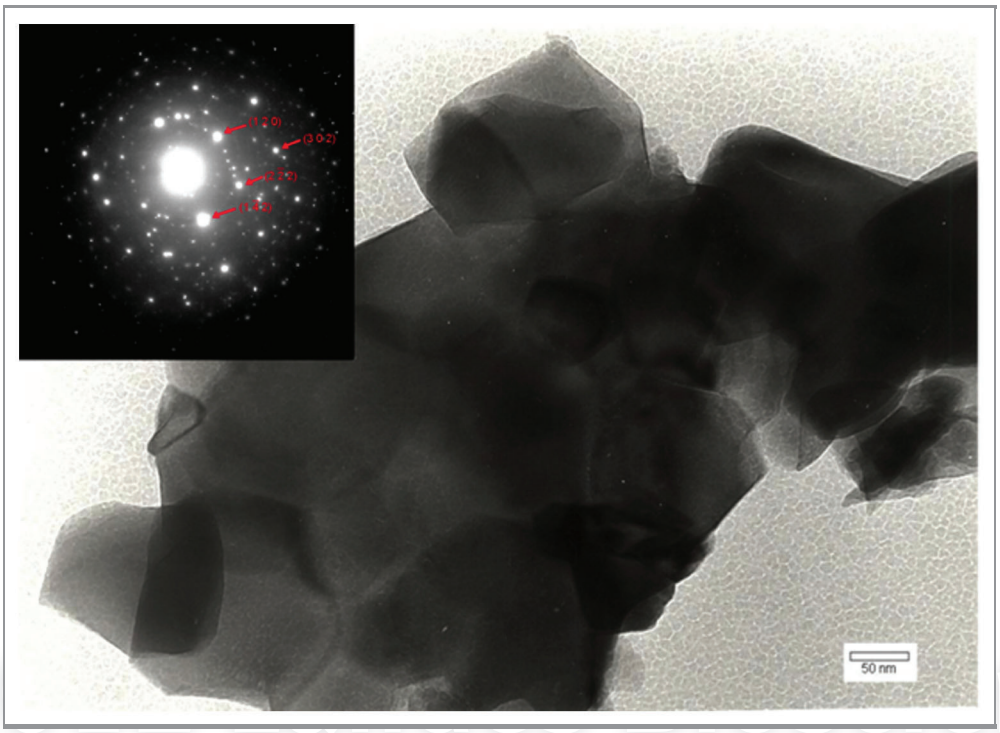

Figure 5. TEM bright field image and electron diffraction for the HA heat-treated at 900°C.

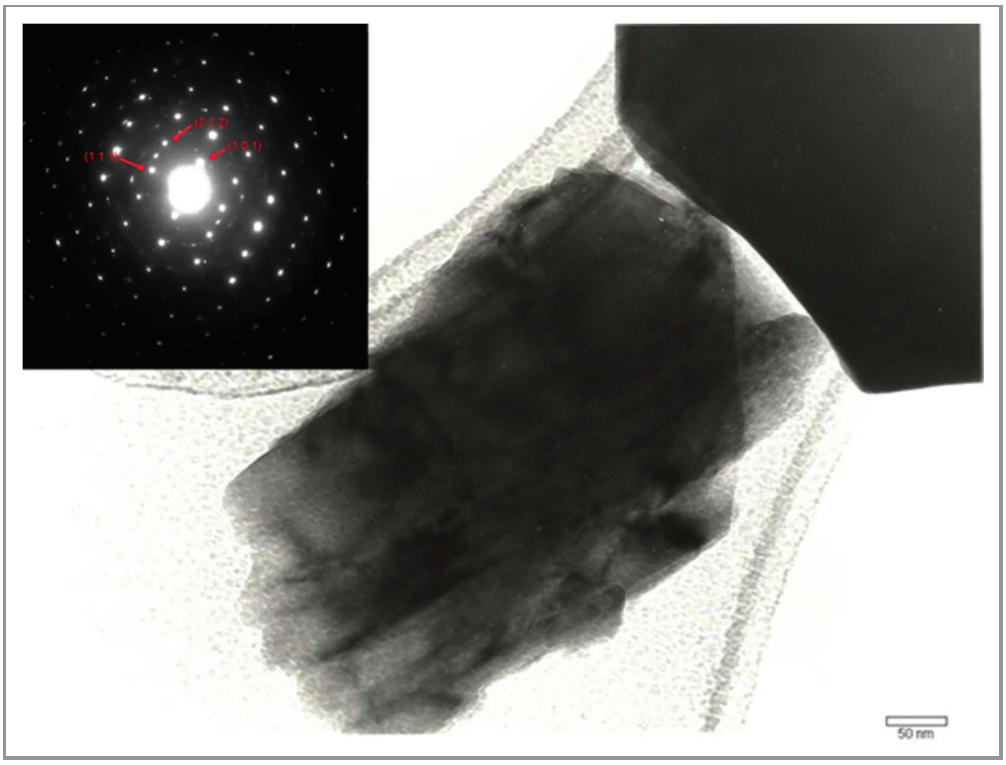

Figure 6. TEM bright field image and electron diffraction for the HA heat-treated at 1,200°C.

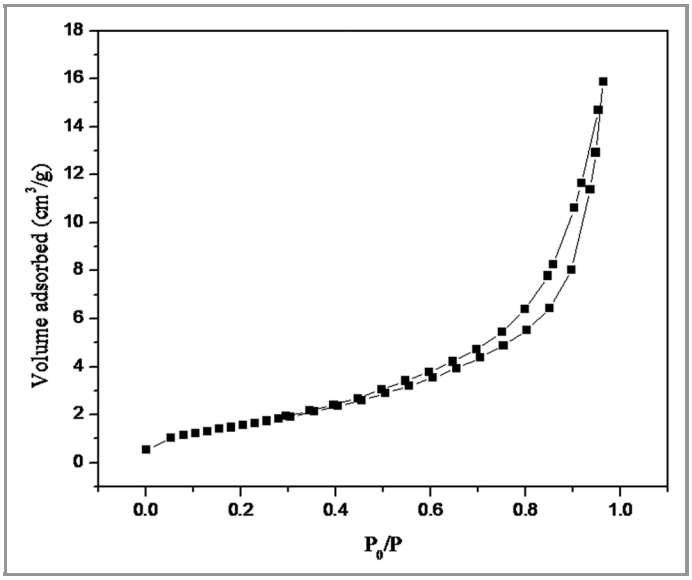

Figure 7. Isotherm adsorption of the nHA sample heat-treated at 600°C.

sharper. The width of the diffraction peaks could be related with the crystal size, which means that the crystal size of the system increases as the heat treatment temperature rises, as can be confirmed by the TEM images.

The electron diffraction pattern for the sample heat-treated at 600°C consists in concentric rings that correspond to nHA phase and are characteristic of nanocrystalline materials with different orientations. In the sample heat-treated at 900°C the electron diffraction pattern consist in spots that correspond to nHA phase but are still present in some rings indicating the presence of some crystals with different orientations, as mentioned above. However, the sample heat-treated a 1,200°C displayed a well-defined spot corresponding to a more ordered atomic array.

It can be observed from **Figure 4** that the grain size is between 10 and 50 nm and the shape of the crystals is rather homogeneous and the TEM pattern, mentioned above, confirms this observation. However, for the samples heat-treated at 900°C and 1200°C, the grain size increased considerably (up to 500 nm), since the energy required for the breaking the barrier of these particles is overcome, producing bigger particles (**Figs. 5 and 6**); giving TEM patterns with higher degree of structural order.

According to IUPAC pore size classification, there are six kinds of adsorption isotherms. Type II isotherm in the classification of Brunauer, Deming and Teller is associated with macroporous solids (more than 50 nm) or non-porous materials. The isotherm adsorption of all samples reported in this work was type II. The surface area values decreased from 7.0 to 2.3 m^2/g as a function of the heat treatment due to crystal growth. These magnitudes would generally classify this material as low-specific-surface-area materials, which are composed of nanoscaled pores.

We speculate that the combination of the nano and macro pores, obtained in this work, will provide a material that could be tested as a plausible material for bone ingrowth. It is believe that the networks surface areas, which provides an advantage toward supplying greater interfacial contact between implant and host tissue, thus improving adhesion and fixation of the implants and, consequently, reducing the chances of implant mobility.

Experimental Process

The synthesis of nHA crystals was performed by sol-gel processing, the chemical reagents were: tetrahydrated calcium nitrate [$Ca(NO_3)_2{\cdot}4H_2O$] and pentoxide phosphorous [P_2O_5]. They were combined in a stoichiometric ratio, as follows: Ca/p = 1.67 (1).

The modified synthesis process consisted of the following steps: (1) solution, (2) mixture, (3) drying and (4) heat treatment. Two different solutions were processed separately; 4.26 g of P_2O_5 reagent were dissolved in 87.6 ml of ethanol to produce a solution at 0.4 M and 23.6 g of $Ca(NO_3)_2$ $4H_2O$ were dissolved in 291.95 ml of ethanol in order to produce a 0.35 M solution.

Once having these two homogeneous solutions, the procedure to mix both solutions consisted in adding the first solution to the second solution in a drop wise fashion, at a rate of 10 ml/min. The final solution was kept under stirring for an hour at room temperature. After this, the mixture was dried at 56°C for 12 h, and then the crystals obtained were ground and heat-treated at 600°C, 900°C and 1,200°C for 2 h. These temperatures were chosen in order to analyze systematically the effect of the temperature on the crystal growth of the nHA formed from the final

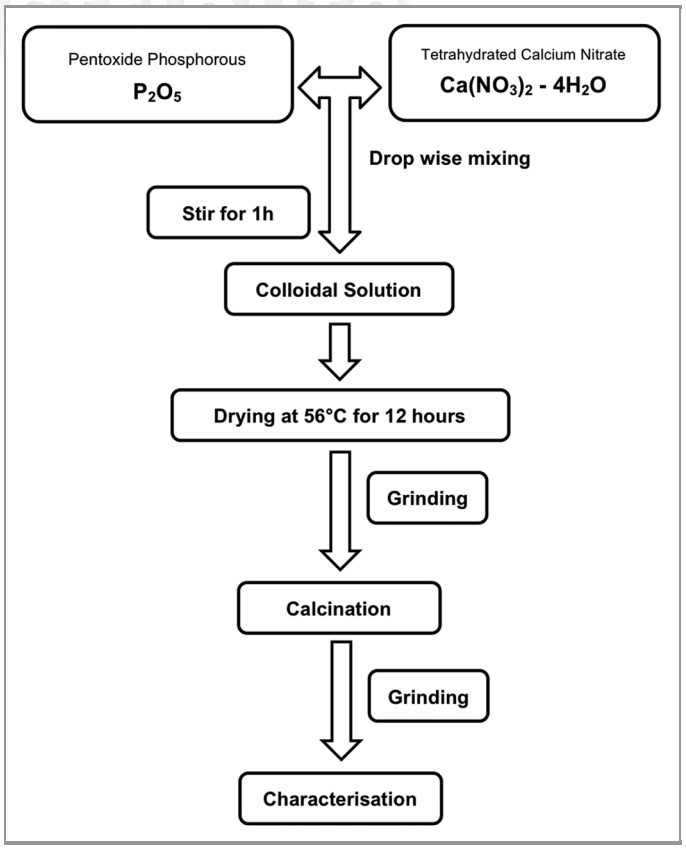

Figure 8. Schematic flow diagram of the experimental process.

solution. The powders obtained were characterized before and after the heat treatment, by means of XRD with a Bruker AXS Diffract plus/D8 Advance diffractometer with CuKα (λ = 0.154 nm), scanning electron microscopy (SEM) with a Leica stereoscan 440 and transmission electron microscopy (TEM) with a JEOL-JEM 1200EX. The specific average surface area of nanopowders was measured from Nitrogen adsorption-desorption isotherms with a Bel-Japan Minisorp II instrument at 77 K using a multi-point technique. Prior to the analysis, the adsorbed moisture on the fine powder surface was eliminated by evaporating at 100°C for 6 h in vacuum, then the surface area was determined by the BET method. It is worth mentioning that three samples were analyzed per each condition and the statistical error was included within the results. A flowchart drawing of the experiment circuit diagram is shown in **Figure 8**.

Conclusions

The experimental method reported in this work can be used to obtain hydroxyapatite nanocrystals within a total process time of less than 16 hours. The size of the crystals obtained ranged from 40 to 500 nm for heat-treating temperatures of 600°C and 1,200°C, respectively. This indicates that the heat-treating temperature may control the crystal size. BET analysis confirmed that the surface area values decreased from 7.0 to 2.3 m^2/g as a function of the heat treatment. The sample heat-treated at 600°C showed a TEM pattern with concentric rings, which is characteristic for crystalline materials having crystals with different orientations. However, as the temperature of the heat treatment increased, the growth of these nHA was promoted and a higher degree of structural order was observed, since the increase of thermal energy allows the system to achieve a more stable configuration.

Disclosure of Potential Conflicts of Interest

No potential conflicts of interest were disclosed.

Acknowledgments

The authors acknowledge the financial support by DGAPA at the National Autonomous University of Mexico through projects IT-104011, IA1101111 and IB100712. Dr H. Pffeifer, MC Adriana Tejeda and Sr Eduardo Antonio Caballero are also acknowledged by their technical support.

References

1. Schumacher M, Deisinger U, Detsch R, Ziegler G. Indirect rapid prototyping of biphasic calcium phosphate scaffolds as bone substitutes: influence of phase composition, macroporosity and pore geometry on mechanical properties. J Mater Sci Mater Med 2010; 21:3119-27; PMID:20953674; http://dx.doi.org/10.1007/s10856-010-4166-6
2. Dorozhkin SV. Calcium orthophosphate based biocomposites and hybrid materials. J Mater Sci 2009; 44:2343-87; http://dx.doi.org/10.1007/s10853-008-3124-x
3. Vitale-Brovarone C, Baino F, Verné E. High strength bioactive glass-ceramic scaffolds for bone regeneration. J Mater Sci Mater Med 2009; 20:643-53; PMID:18941868; http://dx.doi.org/10.1007/s10856-008-3605-0
4. Hesaraki S, Safari M, Shokrgozar MA. Composite bone substitute materials based on beta tricalcium phosphate and magnesium containing sol-gel derived bioactive glass. J Mat Sc Mat in Medicine 2009; 202:2011-7.
5. Sakamoto M. Developed and evaluation of superporous hydroxyapatite ceramics with triple pore structure as bone tissue scaffold. J Ceram Soc Jpn 2010; 118:753-7; http://dx.doi.org/10.2109/jcersj2.118.753
6. Pelin IM, Maier SS, Chitanu GC, Bulacovschi V. Preparation and characterization of a hydroxyapatite-collagen composite as component for injectable bone substitute. Mat Sc Eng C- Mat for Biol App 2009; 29:2188-94; http://dx.doi.org/10.1016/j.msec.2009.04.021
7. Saikia KC, Bhattacharya TD, Bhuyan SK, Talukdar DJ, Saikia SP, Jitesh P. Calcium phosphate ceramics as bone graft substitutes in filling bone tumor defects. Indian J Orthop 2008; 42:169-72; PMID:19826522; http://dx.doi.org/10.4103/0019-5413.39588
8. Faldini C, Moroni A, Giannini S. Hydroxyapatite coated total hip protheses: A long term, prospective, randomized study of 50 consecutive cases. Bioceramics 2002; 218:491-3.
9. Simunek A, Vokurkova J, Kopecka D, Celko M, Mounajjed R, Krulichova I, et al. Evaluation of stability of titanium and hydroxyapatite-coated osseointegrated dental implants: a pilot study. Clin Oral Implants Res 2002; 13:75-9; PMID:12005148; http://dx.doi.org/10.1034/j.1600-0501.2002.130109.x
10. Nair MB, Varma HK, Menon KV, Shenoy SJ, John A. Reconstruction of goat femur segmental defects using triphasic ceramic-coated hydroxyapatite in combination with autologous cells and platelet-rich plasma. Acta Biomater 2009; 5:1742-55; PMID:19297259; http://dx.doi.org/10.1016/j.actbio.2009.01.009
11. Nair MB, Varma HK, John A. Platelet-rich plasma and fibrin glue-coated bioactive ceramics enhance growth and differentiation of goat bone marrow-derived stem cells. Tissue Eng Part A 2009; 15:1619-31; PMID:19072085; http://dx.doi.org/10.1089/ten.tea.2008.0229
12. Yamamiya K, Okuda K, Kawase T, Hata K, Wolff LF, Yoshie H. Tissue-engineered cultured periosteum used with platelet-rich plasma and hydroxyapatite in treating human osseous defects. J Periodontol 2008; 79:811-8; PMID:18454659; http://dx.doi.org/10.1902/jop.2008.070518
13. Okuda K, Tai H, Tanabe K, Suzuki H, Sato T, Kawase T, et al. Platelet-rich plasma combined with a porous hydroxyapatite graft for the treatment of intrabony periodontal defects in humans: a comparative controlled clinical study. J Periodontol 2005; 76:890-8; PMID:15948682; http://dx.doi.org/10.1902/jop.2005.76.6.890
14. Krisanapiboon A, Buranapanitkit B. Biocompatibility of hydroxyapatite composite as a local drug delivery system. J Orthop Surg 2006; 14:315-8.
15. Murugan R, Ramakrishna S. Porous bovine hydroxyapatite for drug delivery. J Appl Biomater Biomech 2005; 3:93-7; PMID:20799228
16. Liu J, Ye X, Wang H, Zhu M, Wang B, Yan H. The influence of pH and temperature on the morphology of hydroxyapatite synthesized by hydrothermal method. Ceram Int 2003; 29:629-33; http://dx.doi.org/10.1016/S0272-8842(02)00210-9
17. Verron E, Khairoun I, Guicheux J, Bouler JM. Calcium phosphate biomaterials as bone drug delivery systems: a review. Drug Discov Today 2010; 15:547-52; PMID:20546919; http://dx.doi.org/10.1016/j.drudis.2010.05.003
18. Saeri MR, Afshara A, Ghorbania M, Ehsania N, Sorrell CC. The wet precipitation process of hydroxyapatite. Mater Lett 2003; 57:4064-9; http://dx.doi.org/10.1016/S0167-577X(03)00266-0
19. Afshara A, Ghorbani M, Ehsania N, Saeria MR, Sorrell CC. Some important factors in the M. wet precipitation process of hydroxyapatite. Mater Des 2003; 24:197-202; http://dx.doi.org/10.1016/S0261-3069(03)00003-7
20. Wang P, Li C, Gong H, Jiang X, Wang H, Li K. Effects of synthesis conditions on the morphology of hydroxyapatite nanoparticles produced by wet chemical process. Powder Technol 2010; 203:315-21; http://dx.doi.org/10.1016/j.powtec.2010.05.023
21. Kuriakosea TA, Kalkura SN, Palanichamyc M, Arivuolid D, Dierkse K, Bocellif G, et al. Synthesis of stoichiometric nanocrystalline hydroxyapatite by ethanol-based sol–gel technique at low temperature. J Cryst Growth 2004; 263:517-23; http://dx.doi.org/10.1016/j.jcrysgro.2003.11.057
22. Guzmán V, Piña-B C, Munguía N. Stoichiometric hydroxyapatite obtained by precipitation and sol gel processes. Rev Mex Fis 2005; 51:284-93.
23. Lewis JA. Colloidal Processing of Ceramics. J Am Ceram Soc 2000; 83:2341-59; http://dx.doi.org/10.1111/j.1151-2916.2000.tb01560.x